Mixed-Valence Compounds

DOI: 10.1002/anie.201406443

Three Distinct Redox States of an Oxo-Bridged Dinuclear Ruthenium Complex**

*Masaki Yoshida, Mio Kondo, Toshikazu Nakamura, Ken Sakai, and Shigeyuki Masaoka**

Abstract: *A series of [{(terpy)(bpy)Ru}(μ-O){Ru(bpy)-(terpy)}]$^{n+}$ (**[RuORu]$^{n+}$**, terpy = 2,2′;6′,2″-terpyridine, bpy = 2,2′-bipyridine) was systematically synthesized and characterized in three distinct redox states (n = 3, 4, and 5 for $Ru^{II,III}{}_2$, $Ru^{III,III}{}_2$, and $Ru^{III,IV}{}_2$, respectively). The crystal structures of **[RuORu]$^{n+}$** (n = 3, 4, 5) in all three redox states were successfully determined. X-ray crystallography showed that the Ru–O distances and the Ru-O-Ru angles are mainly regulated by the oxidation states of the ruthenium centers. X-ray crystallography and ESR spectra clearly revealed the detailed electronic structures of two mixed-valence complexes, **[Ru^{III}ORu^{IV}]$^{5+}$** and **[Ru^{II}ORu^{III}]$^{3+}$**, in which each unpaired electron is completely delocalized across the oxo-bridged dinuclear core. These findings allow us to understand the systematic changes in structure and electronic state that accompany the changes in the redox state.*

Mixed-valence (MV) complexes are excellent model systems for the investigation of electron-transfer phenomena in biophysical processes such as photosynthesis and in artificial electronic devices based on conjugated materials.[1] A pioneering example of an MV compound is the dinuclear Ru complex $[(H_3N)_5Ru^{II}(\mu\text{-pz})Ru^{III}(NH_3)_5]^{5+}$ (pz = pyrazine), the so-called "Creutz–Taube ion," in which the charge is completely delocalized across the dinuclear core.[2] Following the discovery of the Creutz–Taube ion, numerous dinuclear MV complexes have been reported over the past decades.[3,4]

Given that the electronic properties of MV states could be strictly controlled by the oxidation state of the dinuclear core, systematic investigations on the several oxidation states of dinuclear metal complexes are an interesting and important research topic. In principle, dinuclear MV complexes in two different oxidation states can be simply prepared by one-electron oxidation or reduction of their corresponding homovalent compounds (Figure 1). However, although studies on dinuclear MV complexes are abundant, there have been no reports of the isolation and structural determination of a dinuclear metal complex in such three oxidation states, including two different MV states, with the same molecular framework. Such systematic investigation would provide a comprehensive understanding of the structures and properties in conjunction with the oxidation states.

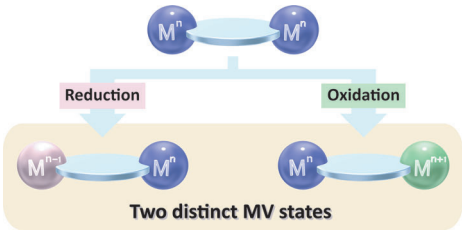

Figure 1. Two distinct MV states derived from a homovalent dimer.

We report herein the syntheses and structures of the three distinct redox states of an oxo (O^{2-})-bridged dinuclear ruthenium complex, [{(terpy)(bpy)Ru}(μ-O){Ru(bpy)-(terpy)}]$^{n+}$ (**[Ru^{II}ORu^{III}]$^{3+}$**, **[Ru^{III}ORu^{III}]$^{4+}$**, and **[Ru^{III}ORu^{IV}]$^{5+}$** for $n = 3$, 4, and 5, respectively; terpy = 2,2′;6′,2″-terpyridine, bpy = 2,2′-bipyridine). Two MV complexes, **[Ru^{III}ORu^{IV}]$^{5+}$** and **[Ru^{II}ORu^{III}]$^{3+}$**, were synthesized by the one-electron oxidation or reduction, respectively, of a homovalent complex, **[Ru^{III}ORu^{III}]$^{4+}$**. Unpaired electrons in **[Ru^{III}ORu^{IV}]$^{5+}$** and **[Ru^{II}ORu^{III}]$^{3+}$** were observed to be fully delocalized across the dinuclear cores.

As a strategy to access two distinct MV states within the same molecular framework, we focused on dinuclear metal complexes bearing a μ-oxo-bridging ligand because these complexes often exhibit multiple well-defined redox process-

[*] Dr. M. Yoshida,[+] Dr. M. Kondo, Prof. T. Nakamura, Prof. S. Masaoka
Institute for Molecular Science (IMS)
5-1 Higashiyama, Myodaiji, Okazaki, Aichi 444-8787 (Japan)
E-mail: masaoka@ims.ac.jp
Dr. M. Yoshida,[+] Prof. K. Sakai
Department of Chemistry, Faculty of Science, Kyushu University
6-10-1 Hakozaki, Higashi-ku, Fukuoka 812-8581 (Japan)
Dr. M. Kondo
ACT-C, Japan Science and Technology Agency (JST)
4-1-8 Honcho, Kawaguchi, Saitama 332-0012 (Japan)
Prof. K. Sakai
WPI-I2CNER and CMS, Kyushu University
744 Motooka, Nishi-ku, Fukuoka 819-0395 (Japan)
[+] Current address: Department of Chemistry
Faculty of Science, Hokkaido University
North-10 West-8, Kita-ku, Sapporo 060-0810 (Japan)

[**] This work was supported by a Grant-in-Aid for Young Scientists (A) (No. 25708011; to S.M.), a Grant-in-Aid for Challenging Exploratory Research (No. 26620160; to S.M.), a Grant-in-Aid for Young Scientists (B) (No. 24750140; to M.K.), and a Grant-in-Aid for Young Scientists (Start-up) (No. 25888023; to M.Y.) from the Japan Society for the Promotion of Science. This work was also supported by a Grant-in-Aid for Scientific Research on Innovative Areas "AnApple" (No. 25107526). M.Y. is grateful to the Research Fellowships of the Japan Society for the Promotion of Science for Young Scientists (No. 223656). The computations were performed using the Research Center for Computational Science, Okazaki (Japan). The authors thank Prof. Hidehiro Sakurai and Mr. Yuki Okabe [Institute for Molecular Science (Japan)] for the measurement of UV-visible-NIR absorption spectra.

Supporting information for this article is available on the WWW under http://dx.doi.org/10.1002/anie.201406443.

es and interesting electronic structures that arise from an electronic coupling between metal ions across the μ-oxo bridge as demonstrated by Meyer et al.[5]

$[Ru^{III}ORu^{III}]^{4+}$ was synthesized by the reaction of [Ru(terpy)(bpy)(OH_2)](NO_3)$_2$ (**$[Ru^{II}OH_2](NO_3)_2$**) with 1.25 equiv of $Ce^{IV}(NH_4)_2(NO_3)_6$ in an aqueous 1M nitric acid solution (Scheme 1, yield: 51%). Notably, the highly soluble

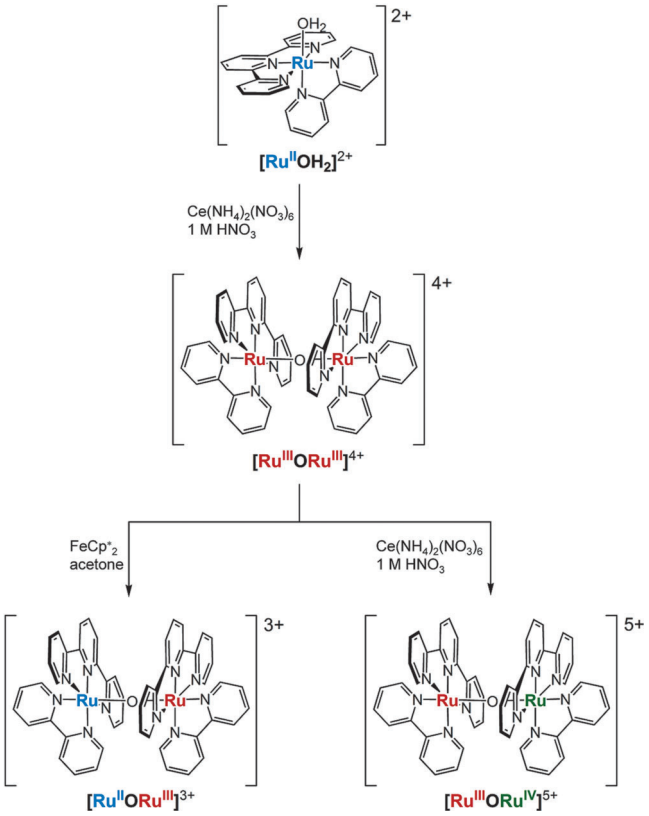

Scheme 1. Syntheses of oxo-bridged dinuclear complexes.

NO_3^- salt of **$[Ru^{II}OH_2]^{2+}$** was employed as a starting material because the formation of the Ru–O–Ru core through dimerization requires a high concentration. The obtained homovalent dimer was characterized by elemental analysis, electrospray ionization time-of-flight mass spectroscopy (ESI-TOF MS), and X-ray crystallography.

In the electrochemical measurements of **$[Ru^{III}ORu^{III}]^{4+}$**, the reversible waves, which correspond to the $Ru^{III,IV}{}_2/Ru^{III,III}{}_2$ couple, were observed in both aqueous (1.265 V vs. NHE at pH 5.31, Figure S1) and dry acetonitrile (1.415 V vs. NHE, Figures S2 and S3) solution. By contrast, the redox peak assigned to the reduction of $Ru^{III,III}{}_2$ to $Ru^{II,III}{}_2$ was observed as an irreversible wave in aqueous solution (0.324 V), although that in acetonitrile was reversible (0.486 V). This irreversible wave in an aqueous solution indicates that the one-electron reduced species **$[Ru^{II}ORu^{III}]^{3+}$** rapidly decomposes into a monomeric complex in aqueous solution.[5a,e,f]

The aforementioned results encouraged us to synthesize MV complexes by one-electron oxidation and reduction of **$[Ru^{III}ORu^{III}]^{4+}$**. In fact, we successfully synthesized **$[Ru^{III}ORu^{IV}]^{5+}$** by reacting in situ-generated **$[Ru^{III}ORu^{III}]^{4+}$** with an excess amount of $Ce^{IV}(NH_4)_2(NO_3)_6$ ($E_0 = 1.61$ V in an aqueous 1M HNO_3) in an aqueous 1M nitric acid solution with 75% yield (Scheme 1). **$[Ru^{III}ORu^{III}]^{4+}$** was reduced by 1 equiv of decamethylferrocene ($E_0 = 0.07$ V) in an organic medium, and the one-electron-reduced **$[Ru^{II}ORu^{III}]^{3+}$** was obtained in 60% yield. Notably, strict inert conditions were required for the preparation of **$[Ru^{II}ORu^{III}]^{3+}$** to avoid the decomposition of the Ru^{II}–O–Ru^{III} core by water,[5a,e,f] as evidenced by electrochemical measurements.

We successfully determined the crystal structures of **$[RuORu]^{n+}$** in all three redox states ($n = 3$, 4, 5), as shown in Figure 2.[6] The coordination geometry at each Ru atom is

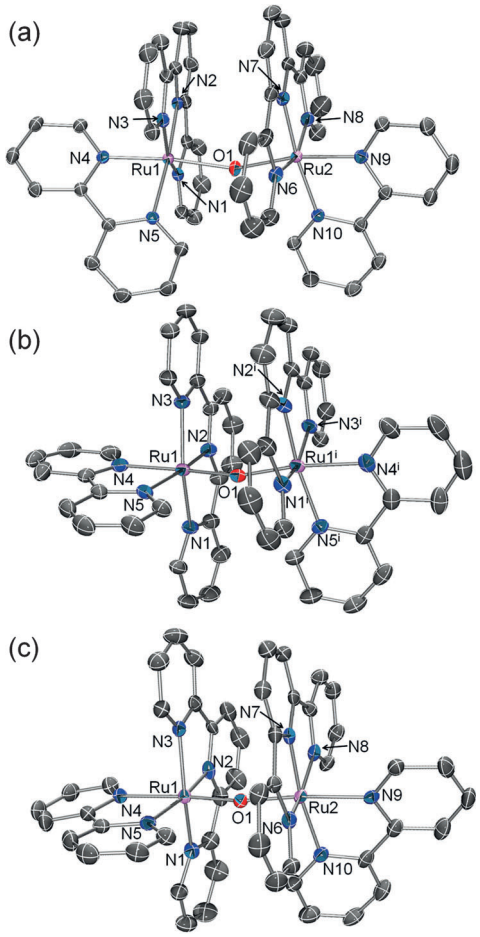

Figure 2. The structures of the cationic part of a) **$[Ru^{II}ORu^{III}]$**-$(ClO_4)_3$·$MeNO_2$·PhMe, b) **$[Ru^{III}ORu^{III}](ClO_4)_4$**·3 $MeNO_2$, and c) **$[Ru^{III}ORu^{IV}](ClO_4)_5$**·$NaClO_4$·3 H_2O, showing the atom-labeling scheme. Thermal ellipsoids are displayed at the 50% probability level. H atoms have been omitted for clarity. The crystallographic data are summarized in Table S6.

that of a distorted octahedron composed of a meridionally coordinated terpyridine ligand, a bidentate bipyridine ligand, and a bridging oxo ligand, irrespective of the oxidation state. For **$[Ru^{III}ORu^{III}]^{4+}$**, three different crystal structures were obtained with different combinations of counteranions and solvated molecules (**$[Ru^{III}ORu^{III}](ClO_4)_4$**·3 $MeNO_2$, **$[Ru^{III}ORu^{III}](ClO_4)_4$**·2 MeCN, and **$[Ru^{III}ORu^{III}]$**-

$(NO_3)_4 \cdot 2MeCN$; Figures 2 and S4), in which the Ru–O distance (ca. 1.88 Å) and Ru-O-Ru angles (ca. 163°) are similar in all of the $[Ru^{III}ORu^{III}]^{4+}$ structures. By contrast, the Ru–O distances and Ru-O-Ru angles largely depend on the oxidation states of the Ru atoms. The Ru–O bonds of $[Ru^{III}ORu^{IV}]^{5+}$ (ca. 1.84 Å) are considerably shorter compared with those of $[Ru^{III}ORu^{III}]^{4+}$ (ca. 1.88 Å), and the Ru-O-Ru angle (170.64(15)°) is much larger than that of $[Ru^{III}ORu^{III}]^{4+}$ (ca. 163°), as shown in Figure 3 and

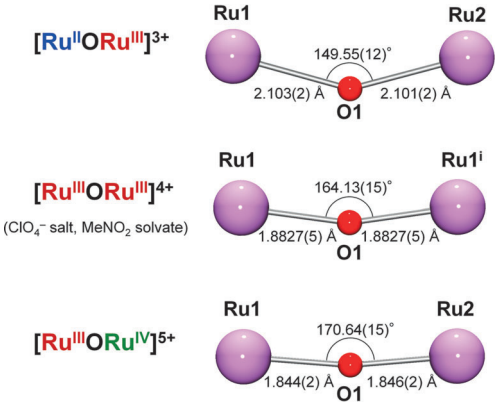

Figure 3. Comparison of the structure of the Ru–O–Ru core of the complex in each oxidation state.

Table S1. In the case of $[Ru^{II}ORu^{III}]^{3+}$, the opposite trend was observed: the Ru–O bonds are longer (ca. 2.10 Å) and the Ru-O-Ru angle is smaller (149.55(12)°) compared with those of $[Ru^{III}ORu^{III}]^{4+}$. For both MV complexes, $[Ru^{III}ORu^{IV}]^{5+}$ and $[Ru^{II}ORu^{III}]^{3+}$, the two Ru–O bonds are almost identical, which indicates that the two Ru centers are almost equivalent and that the charge of these complexes is delocalized along the Ru–O–Ru core (Figure 3, Table S1).

The UV-visible absorption spectra of $[Ru^{III}ORu^{III}]^{4+}$, $[Ru^{II}ORu^{III}]^{3+}$, and $[Ru^{III}ORu^{IV}]^{5+}$ are shown in Figure 4a. The spectra of all the complexes exhibit intense absorption bands in the UV region, corresponding to the ligand-based π–π* transitions. Additionally, a moderately intense band centered at 686 nm ($\varepsilon = 2.37 \times 10^4\,M^{-1}cm^{-1}$) was observed in the spectrum of $[Ru^{III}ORu^{III}]^{4+}$. Time-dependent DFT (TD-DFT) calculations performed using the UB3LYP/LandL2DZ basis sets indicate that the band can be assigned mainly to the transition from $d\pi^{nb}$(Ru–O–Ru) to $d\pi^*$(Ru–O–Ru) ($\lambda_{calcd} =$ 634.4 nm, $f = 0.245$, HOMO-1→LUMO; see Figures 4b and S6 and Table S2). The spectrum of $[Ru^{III}ORu^{IV}]^{5+}$ shows a moderately intense band centered at 479 nm ($\varepsilon = 2.22 \times 10^4\,M^{-1}cm^{-1}$, Figure 4a), which is attributed to the transition from molecular orbitals containing $d\pi^{nb}$(Ru–O–Ru) character to the orbital of $d\pi^*$(Ru–O–Ru), as evidenced by TD-DFT calculations ($\lambda_{calcd} = 444.66$ ($f = 0.1234$), 503.42 ($f =$ 0.1063), and 523.87 nm ($f = 0.0964$); see Figures 4b and S7 and Table S3). No absorption band was observed in the near-IR region (1000–1800 nm, Figure S5). The spectrum of $[Ru^{II}ORu^{III}]^{3+}$ displays a moderately intense band centered at 841 nm ($\varepsilon = 1.21 \times 10^4\,M^{-1}cm^{-1}$). TD-DFT calculations showed that the band at approximately 841 nm is mainly

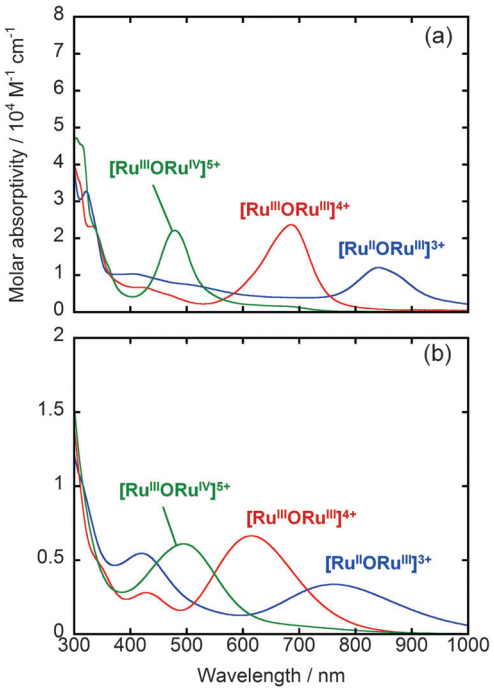

Figure 4. a) The UV-visible absorption spectrum of $[Ru^{II}ORu^{III}]^{3+}$ in dry acetonitrile at 20 °C under an Ar atmosphere (blue line) and the spectra of $[Ru^{III}ORu^{III}]^{4+}$ (red line) and $[Ru^{III}ORu^{IV}]^{5+}$ (green line) in aqueous 0.5 M sulfuric acid solutions (pH 0.51) at 20 °C in air. b) The UV-visible absorption spectra simulated on the basis of the TD-DFT calculations for $[Ru^{II}ORu^{III}]^{3+}$ (blue line; triplet, in acetonitrile), $[Ru^{III}ORu^{III}]^{4+}$ (red line; open-shell singlet, in water), and $[Ru^{III}ORu^{IV}]^{5+}$ (green line; triplet, in water).

composed of the $d\pi^{nb}$(Ru–O–Ru)→$d\pi^*$(Ru–O–Ru) transition ($\lambda_{calcd} = 767.86$ nm, $f = 0.1489$, β-HOMO-1→β-LUMO; see Figures 3b and S8 and Table S4).

X-band ESR and the magnetic susceptibility measurements of $[Ru^{III}ORu^{III}]^{4+}$ and $[Ru^{III}ORu^{IV}]^{5+}$ were carried out to examine their magnetic behaviors.[7] No ESR signals were detected for $[Ru^{III}ORu^{III}]^{4+}$ at 6.9 K (Figure S9), which indicates that the complex is essentially diamagnetic in the ground state. The effective magnetic moment (μ_{eff}) increased with increasing temperature (Figures S10 and S11), and the μ_{eff} value at 300 K (2.39 μ_B) corresponds to 1.6 unpaired electrons per dimer under the assumption that $g = 2$. These values are comparable with those previously reported for Ru^{III}–O–Ru^{III} complexes.[5j,8] This paramagnetism of $[Ru^{III}ORu^{III}]^{4+}$ at 300 K was also confirmed in solution by ^1H NMR spectroscopy. The ESR spectrum of $[Ru^{III}ORu^{IV}]^{5+}$ at 6.9 K gave a broad anisotropic signal with $g = 1.39$, which is attributed to an $S = 1/2$ ground state. This g-value is significantly smaller than that reported for a partially localized Ru^{III}–O–Ru^{IV} system ($g = 1.78$),[9] indicating the occurrence of large spin-orbit coupling in the Ru–O–Ru core. The extrapolated intercept of the μ_{eff} value of $[Ru^{III}ORu^{IV}]^{5+}$ (ca. 0.73 μ_B) is almost consistent with an $S = 1/2$ ground state of $[Ru^{III}ORu^{IV}]^{5+}$.

Our systematic investigation allowed us to elucidate the relationship among the molecular structures, electronic properties, and oxidation states of the oxo-bridged dinuclear

ruthenium complex. In homovalent $[Ru^{III}ORu^{III}]^{4+}$, two unpaired electrons are located on the Ru centers (d^5, low-spin) and interact antiferromagnetically with each other, as suggested by the magnetic susceptibility, ESR, and ^1H NMR spectroscopy results. DFT calculations showed that the unpaired electrons of $[Ru^{III}ORu^{III}]^{4+}$ are incorporated into antibonding dπ*(Ru–O–Ru) orbitals, which are formed through the dπ–pπ–dπ interaction between the p orbitals of the O and the dπ orbitals of the Ru (Scheme 2 and Figure S6).

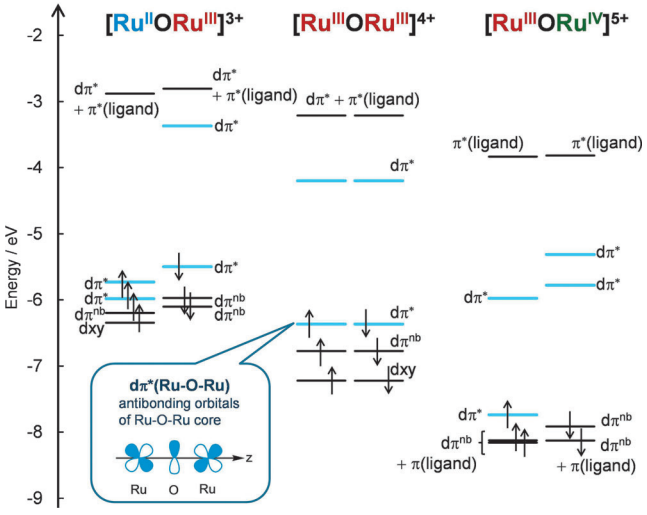

Scheme 2. MO diagram for a Ru–O–Ru core. Orbitals represented as blue lines are dπ* orbitals of a Ru–O–Ru core.

Because both the HOMO and the LUMO of $[Ru^{III}ORu^{III}]^{4+}$ are assigned to the antibonding dπ*(Ru–O–Ru) orbitals, the Ru–O–Ru core exhibits multibonding character along the Ru–O–Ru axes; the bond order for each Ru–O bond was determined to be 1.5. One-electron oxidation of $[Ru^{III}ORu^{III}]^{4+}$ corresponds to the removal of one electron from an antibonding dπ*(HOMO) orbital, thus increasing the bond order of the Ru–O bond to 1.75. In fact, X-ray structural analysis revealed that the Ru–O bonds and Ru–O–Ru angle of $[Ru^{III}ORu^{IV}]^{5+}$ are shorter and larger, respectively, than those of $[Ru^{III}ORu^{III}]^{4+}$, which reflects the strengthening of the multiple-bonding character of the Ru–O–Ru core. By contrast, a one-electron reduction of $[Ru^{III}ORu^{III}]^{4+}$ corresponds to the addition of one electron to an antibonding dπ*(LUMO) orbital, thus decreasing the bond order of the Ru–O bond to 1.25. This result is consistent with the fact that the Ru–O bonds and Ru-O-Ru angle of $[Ru^{II}ORu^{III}]^{3+}$ are longer and smaller, respectively, than those of $[Ru^{III}ORu^{III}]^{4+}$, as suggested by the X-ray structural analysis. Notably, the unpaired electrons of $[Ru^{III}ORu^{IV}]^{5+}$ and $[Ru^{II}ORu^{III}]^{3+}$ are completely delocalized along the Ru–O–Ru core, as supported by the X-ray structural analysis, and ESR spectroscopy results.

In the present study, we demonstrated the synthesis and structural determination of the oxo-bridged dinuclear ruthenium complex $[RuORu]^{n+}$ in three distinct oxidation states ($n = 3, 4, 5$). This work is the first report on the structural determination of three successive oxidation states, including two different MV states, of dinuclear metal complexes with the same molecular framework (Figure 1). Moreover, our crystallographic and spectroscopic investigations revealed that $[Ru^{III}ORu^{IV}]^{5+}$ and $[Ru^{II}ORu^{III}]^{3+}$ are completely delocalized MV systems, and the results of UV-visible absorption spectroscopy and TD-DFT calculation also showed the electronic structure of MV complexes in solution. Despite a large number of studies on the synthesis and redox reactions of oxo-bridged dinuclear ruthenium complexes,[5,8–10] to the best of our knowledge, the literature contains only three previous reports on the crystal structures of mixed-valence oxo-bridged dinuclear Ru complexes; furthermore, all three reports are on the partially localized Ru^{III}–O–Ru^{IV} systems.[11] Therefore, $[Ru^{III}ORu^{IV}]^{5+}$ is the first example of a structurally determined fully delocalized Ru^{III}–O–Ru^{IV} system, and $[Ru^{II}ORu^{III}]^{3+}$ is the first structurally determined Ru^{II}–O–Ru^{III} system. Our systematic investigations of the three distinct redox states of an oxo-bridged dinuclear ruthenium complex sheds new light on the electronic state of MV systems and also provides new ideas for controlling metal–metal interactions of materials with multiple metal sites.

Received: June 21, 2014
Revised: July 30, 2014
Published online: September 4, 2014

Keywords: charge distribution · mixed-valence compounds · multiple bonds · ruthenium · μ-oxo complexes

[1] a) G. W. Brudvig, R. H. Crabtree, *Prog. Inorg. Chem.* **1989**, *37*, 99; b) F. Paul, C. Lapinte, *Coord. Chem. Rev.* **1998**, *178–180*, 427.
[2] a) C. Creutz, H. Taube, *J. Am. Chem. Soc.* **1969**, *91*, 3988; b) C. Creutz, H. Taube, *J. Am. Chem. Soc.* **1973**, *95*, 1086; c) C. Creutz, P. C. Ford, T. J. Meyer, *Inorg. Chem.* **2006**, *45*, 7059.
[3] a) K. D. Demadis, C. M. Hartshorn, T. J. Meyer, *Chem. Rev.* **2001**, *101*, 2655; b) B. S. Brunschwig, C. Creutz, N. Sutin, *Chem. Soc. Rev.* **2002**, *31*, 168; c) D. M. D'Alessandro, F. R. Keene, *Chem. Rev.* **2006**, *106*, 2270; d) W. Kaim, G. K. Lahiri, *Angew. Chem. Int. Ed.* **2007**, *46*, 1778; *Angew. Chem.* **2007**, *119*, 1808.
[4] For recent studies: a) B. Bechlars, D. M. D'Alessandro, D. M. Jenkins, A. T. Iavarone, S. D. Glover, C. P. Kubiak, J. R. Long, *Nat. Chem.* **2010**, *2*, 362; b) M. A. Fox, B. Le Guennic, R. L. Roberts, D. A. Brue, D. S. Yufit, J. A. K. Howard, G. Manca, J.-F. Halet, F. Hartl, P. J. Low, *J. Am. Chem. Soc.* **2011**, *133*, 18433; c) C.-J. Yao, Y.-W. Zhong, J. Yao, *J. Am. Chem. Soc.* **2011**, *133*, 15697; d) S. Rodríguez González, M. C. R. Delgado, R. Caballero, P. De La Cruz, F. Langa, J. T. López Navarrete, J. Casado, *J. Am. Chem. Soc.* **2012**, *134*, 5675; e) L. A. Wilkinson, L. McNeill, A. J. H. M. Meijer, N. J. Patmore, *J. Am. Chem. Soc.* **2013**, *135*, 1723; f) M. R. Halvagar, P. V. Solntsev, H. Lim, B. Hedman, K. O. Hodgson, E. I. Solomon, C. J. Cramer, W. B. Tolman, *J. Am. Chem. Soc.* **2014**, *136*, 7269.
[5] a) T. R. Weaver, T. J. Meyer, S. A. Adeyemi, G. M. Brown, R. P. Eckberg, W. E. Hatfield, E. C. Johnson, R. W. Murray, D. Untereker, *J. Am. Chem. Soc.* **1975**, *97*, 3039; b) J. A. Baumann, T. J. Meyer, *Inorg. Chem.* **1980**, *19*, 345; c) S. W. Gersten, G. J. Samuels, T. J. Meyer, *J. Am. Chem. Soc.* **1982**, *104*, 4029; d) K. J. Takeuchi, M. S. Thompson, D. W. Pipes, T. J. Meyer, *Inorg. Chem.* **1984**, *23*, 1845; e) J. A. Gilbert, D. S. Eggleston, W. R. Murphy, D. A. Geselowitz, S. W. Gersten, D. J. Hodgson, T. J.

Meyer, *J. Am. Chem. Soc.* **1985**, *107*, 3855; f) P. Doppelt, T. J. Meyer, *Inorg. Chem.* **1987**, *26*, 2027; g) O. Ishitani, P. S. White, T. J. Meyer, *Inorg. Chem.* **1996**, *35*, 2167; h) E. L. Lebeau, S. A. Adeyemi, T. J. Meyer, *Inorg. Chem.* **1998**, *37*, 6476; i) F. Liu, J. J. Concepcion, J. W. Jurss, T. Cardolaccia, J. L. Templeton, T. J. Meyer, *Inorg. Chem.* **2008**, *47*, 1727; j) J. W. Jurss, J. J. Concepcion, J. M. Butler, K. M. Omberg, L. M. Baraldo, D. G. Thompson, E. L. Lebeau, B. Hornstein, J. R. Schoonover, H. Jude, J. D. Thompson, D. M. Dattelbaum, R. C. Rocha, J. L. Templeton, T. J. Meyer, *Inorg. Chem.* **2012**, *51*, 1345.

[6] CCDC 1009133, 1009134, 1009135, 1009136, and 1009137 for **[$Ru^{II}ORu^{III}$]**$(ClO_4)_3 \cdot MeNO_2 \cdot PhMe$, **[$Ru^{III}ORu^{III}$]**$(ClO_4)_4 \cdot 3\,MeNO_2$, **[$Ru^{III}ORu^{III}$]**$(ClO_4)_4 \cdot 2\,MeCN$, **[$Ru^{III}ORu^{III}$]**$(NO_3)_4 \cdot 2\,MeCN$, and **[$Ru^{III}ORu^{IV}$]**$(ClO_4)_5 \cdot NaClO_4 \cdot 3\,H_2O$, respectively, contain the supplementary crystallographic data for this paper. These data can be obtained free of charge from The Cambridge Crystallographic Data Centre via http://www.ccdc.cam.ac.uk/data_request/cif.

[7] Measurements for **[$Ru^{II}ORu^{III}$]$^{3+}$** were not allowed because of the instability of the sample.

[8] R. Schneider, T. Weyhermüller, K. Wieghardt, B. Nuber, *Inorg. Chem.* **1993**, *32*, 4925.

[9] a) J. A. Stull, R. D. Britt, J. L. McHale, F. J. Knorr, S. V. Lymar, J. K. Hurst, *J. Am. Chem. Soc.* **2012**, *134*, 19973; b) J. A. Stull, T. A. Stich, J. K. Hurst, R. D. Britt, *Inorg. Chem.* **2013**, *52*, 4578.

[10] a) F. P. Rotzinger, S. Munavalli, P. Comte, J. K. Hurst, M. Grätzel, F.-J. Pern, A. J. Frank, *J. Am. Chem. Soc.* **1987**, *109*, 6619; b) H. H. Petach, M. Elliott, *J. Electrochem. Soc.* **1992**, *139*, 2217; c) H. Yamada, W. F. Siems, T. Koike, J. K. Hurst, *J. Am. Chem. Soc.* **2004**, *126*, 9786.

[11] a) J. R. Schoonover, J. Ni, L. Roecker, P. S. White, T. J. Meyer, *Inorg. Chem.* **1996**, *35*, 5885; b) A. D. Ryabov, R. Le Lagadec, H. Estevez, R. A. Toscano, S. Hernandez, L. Alexandrova, V. S. Kurova, A. Fischer, C. Sirlin, M. Pfeffer, *Inorg. Chem.* **2005**, *44*, 1626.

